New Wideband Meta Materials Printed Antennas for Medical Applications

Albert Sabban

Electronic Engineering Department ORT Braude College, Karmiel, Israel, 21982

sabban@netvision.net.il

Abstract

Communication and Biomedical industry is in rapid growth in the last decade. Low profile small antennas are crucial in the development of commercial compact systems. Small printed antennas suffer from low efficiency. Meta material technology is used to design small wideband wearable antennas with high efficiency. Design considerations, computed and measured results of printed metamaterials antennas with high efficiency are presented in this paper. The proposed antenna may be used in Communication and Medicare systems. The antennas S11 results for different positions on the human body are presented in this paper. The gain and directivity of the patch antenna with SRR is higher by 2.5dB than the patch antenna without SRR. The resonant frequency of the antenna with SRR on human body is shifted by 3%.

Keywords

Metamaterial Antennas; Microstrip Antennas

Introduction

Microstrip antennas are widely used in communication systems. Microstrip antennas have several advantages such as low profile, flexible, light weight, small volume and low production cost. Compact printed antennas are presented in journals and books, as referred in [1]-[4]. However, small printed antennas suffer from low efficiency. Meta material technology is used to design small printed antennas with high efficiency. Printed wearable antennas were presented in [5]. Artificial media with negative dielectric permittivity were presented in [6]. Periodic SRR and metallic posts structures may be used to design materials with dielectric constant and permeability less than 1 as presented in [6]-[14]. In this paper meta-material technology is used to develop small antennas with high efficiency. The electrical parameters of wearable antennas are affected by the RF transmission properties of human tissues as presented in [15-16]. Several wearable antennas have been presented in papers in the last years as referred in [17-24]. New wearable printed meta-materials antennas with high efficiency are presented in this paper. The bandwidth of the meta-material antenna with SRR and metallic strips is around 50% for VSWR better than 2.3:1. Analysis computed and measured results of meta-materials antennas are presented in this paper.

New Antenna with Split Ring Resonators

At first a microstrip loaded dipole antenna has been designed to provide horizontal polarization. The second step was to design the same antenna with Split Ring Resonators. The antennas consists of two layers. The first layer consists of RO3035 0.8mm dielectric substrate. The second layer consists of RT-Duroid 5880 0.8mm dielectric substrate. The printed slot antenna provides a vertical polarization. The printed dipole and the slot antenna provide dual orthogonal polarizations. The dimensions of the dual polarized antenna shown in Figure 1 are 26x6x0.16cm. The antenna has been analyzed by using Agilent ADS software. The matching stubs width and length has been optimized to get the best VSWR results at the antenna input ports. The length of the stub L is 10mm. The number and location of the coupling stubs control the axial ratio value. The axial ratio value may vary from 0dB to 20dB due to different location and number of the coupling stubs. The length and width of the coupling stubs in Figure 1 are 12mm by 10mm.The number of coupling stubs may be minimized to around four. The antenna cross polarized field strength may be adjusted by varying the slot feed location. There is a good agreement between measured and computed results.

The antenna bandwidth is around 10% for VSWR better than 2:1. The antenna beam width is around 100º. The

2327-7238/15/01 013-12, © 2015 DEStech Publications, Inc.
doi:10.12783/ams.2015.0301.02

antenna gain is around 2dBi. The computed S11 parameters are presented in Figure 2. Figure 3 presents the antenna measured S11 parameters.

The antenna bandwidth is around 10% for VSWR better than 2:1. The antenna beam width is around 100º.

The antenna size may be reduced by folding the printed dipole as shown in Figure 4. The dimensions of the folded dual polarized antenna presented in Figure 4 are 7x5x0.16cm. The length and width of the coupling stubs in Figure 5 are 12mm by 9mm. Small tuning bars are located along the feed line to tune the antenna to the desired resonant frequency. Figure 5 presents the antenna computed S11 and S22 parameters. The antenna with Split Ring Resonators is shown in Figure 6. The ring width is 1.4mm the spacing between the rings is 1.4mm. The resonant frequency of the antenna with SRR is 400MHz, around 10% lower than the resonant frequency of the antenna without the Split Ring Resonators. The computed S11 parameters are presented in Figure 7. The antenna presented in Figure 6 has been modified as shown in Figure 8. The computed S11 parameters are presented in Figure 9. The modified antenna has two resonant frequencies. The first resonant frequency is 370MHz and is lower by 20% than the resonant frequency of the antenna without the SRR.
Metallic strips have been added to the antenna with SRR as presented in Figure 10. The computed S11 parameter of the antenna with metallic strips is presented in Figure 11.

The antenna bandwidth is around 50% for VSWR better than 3:1. The computed radiation pattern is shown in Figure 12. The 3D computed radiation pattern is shown in Figure 13.

Directivity and gain of the antenna with SRR is around 5dBi as shown in Figure 14. The directivity of a similar antenna without SRR is around 2dBi. The feed network of the antenna presented in Figure 10 has been optimized to yield VSWR better than 2:1 in frequency range of 250MHz to 440MHz.

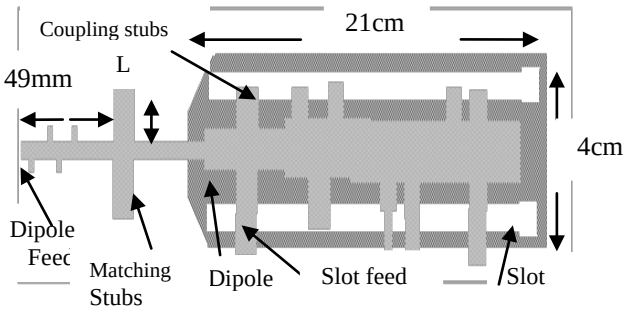

FIGURE 1. PRINTED DUAL POLARIZED ANTENNA, 26X6X0.16 CM.

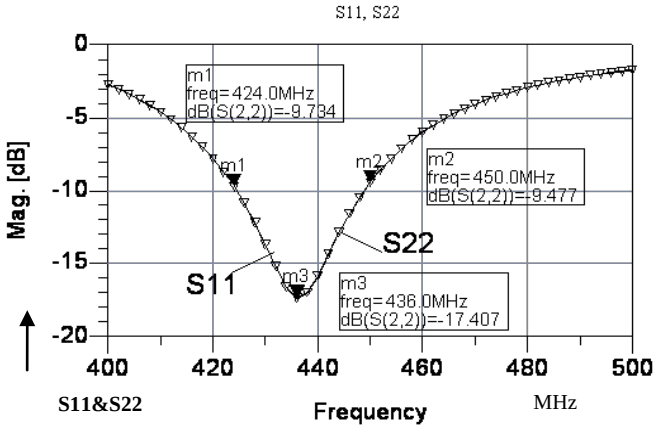

FIGURE 2. COMPUTED S11 AND S22 RESULTS

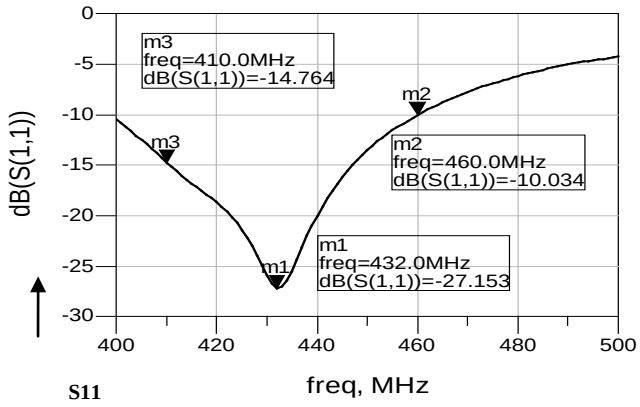

FIGURE 3. MEASURED S11

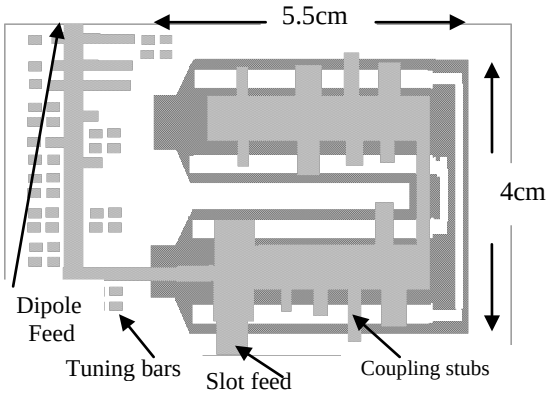

FIGURE 4. FOLDED DUAL POLARIZED ANTENNA, 7X5X0.16CM

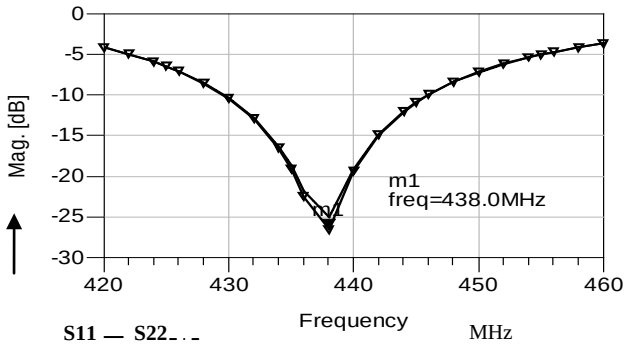

FIGURE 5. FOLDED ANTENNA COMPUTED S11AND S22 RESULTS

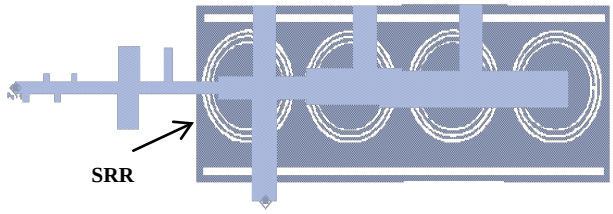

FIGURE 6. PRINTED ANTENNA WITH SPLIT RING RESONATORS

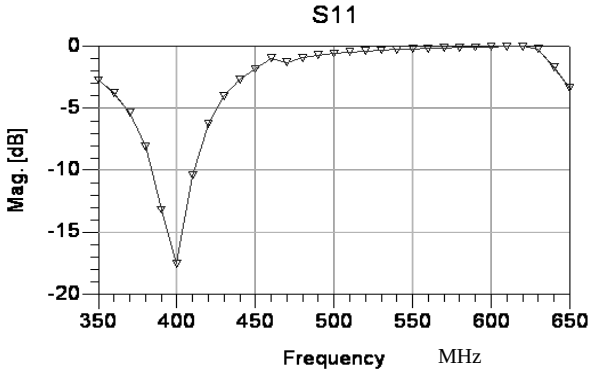

FIGURE 7. ANTENNA WITH SPLIT RING RESONATORS, COMPUTED S11

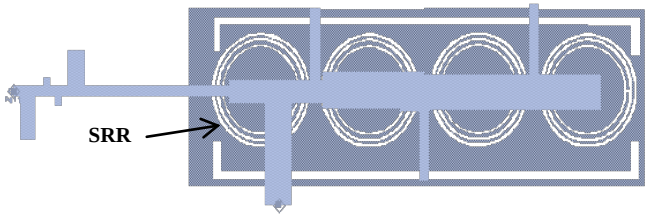

FIGURE 8. ANTENNA WITH SRR WITH TWO RESONANT FREQUENCIES

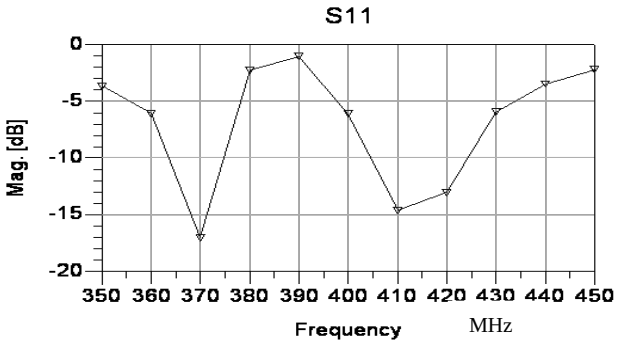

FIGURE 9. S11 FOR ANTENNA WITH TWO RESONANT FREQUENCIES

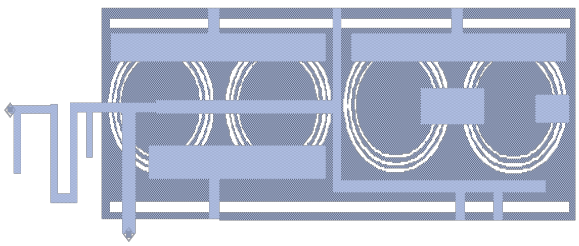

FIGURE 10. ANTENNA WITH SRR AND METALLIC STRIPS

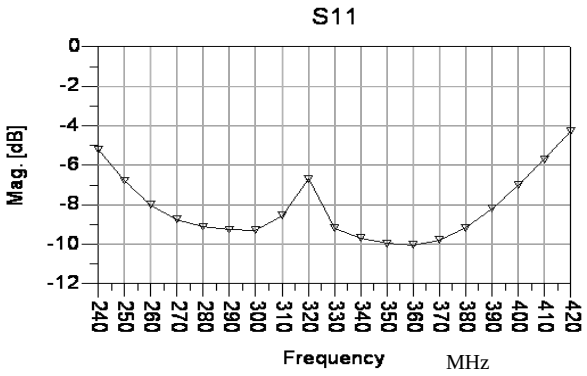

FIGURE 11. S11 FOR ANTENNA WITH SRR AND METALLIC STRIPS

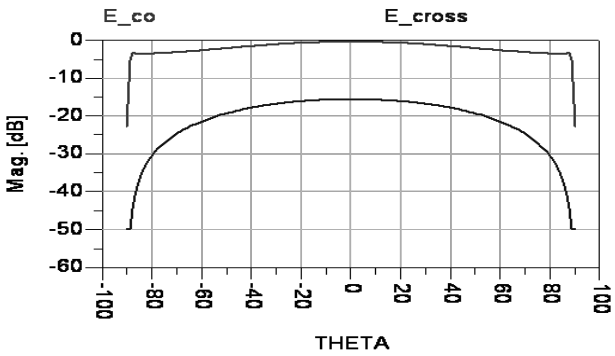

FIGURE 12. RADIATION PATTERN FOR ANTENNA WITH SRR

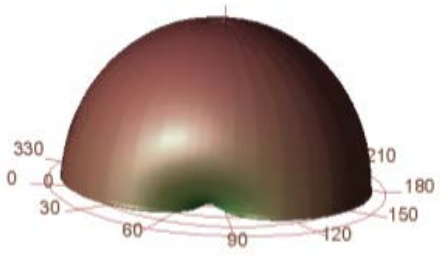

FIGURE 13. 3D RADIATION PATTERN FOR ANTENNA WITH SRR

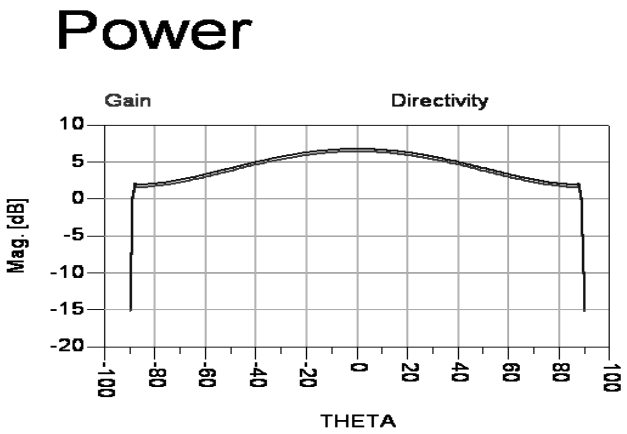

FIGURE 14. DIRECTIVITY OF THE ANTENNA WITH SRR

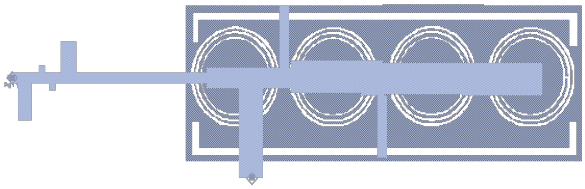

FIGURE 15. ANTENNA WITH SRR WITH TWO COUPLING STUBS

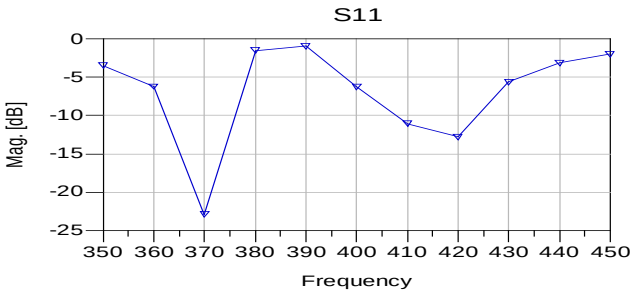

FIGURE 16. S11 FOR ANTENNA WITH SRR WITH TWO COUPLING STUBS

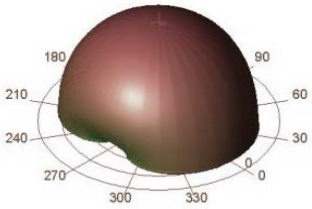

FIGURE 17. 3D RADIATION PATTERN FOR ANTENNA WITH SRR AND TWO COUPLING STUBS

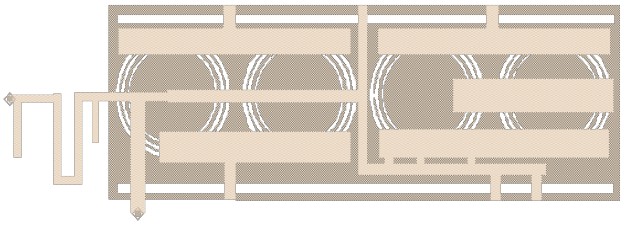

FIGURE 18. WIDEBAND ANTENNA WITH SRR AND METALLIC STRIPS

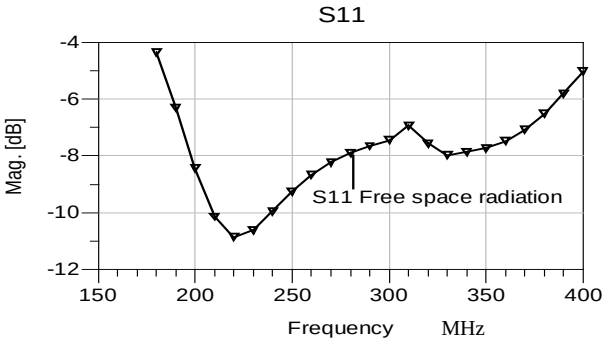

FIGURE 19. S11 FOR ANTENNA WITH SRR AND METALLIC STRIPS

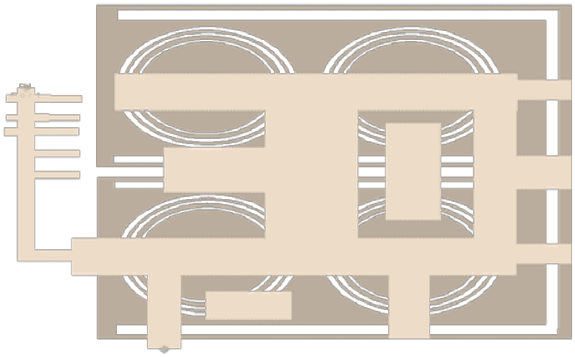

FIGURE 20. FOLDED DUAL POLARIZED ANTENNA WITH SRR

Optimization of the number of the coupling stubs and the distance between the coupling stubs may be used to tune the antenna resonant frequency. An optimized antenna with two coupling stubs has two resonant frequencies. The first resonant frequency is 370MHz and the second resonant frequency is 420MHz. Antenna with SRR with two coupling stubs is presented in Figure 15. The computed S11 parameter of the antenna with two coupling stubs is presented in Figure 16. The 3D Radiation pattern for antenna with SRR and two coupling stubs is shown in Figure 17.

The antenna with metallic strips has been optimized to yield wider bandwidth as shown in Figure 18.

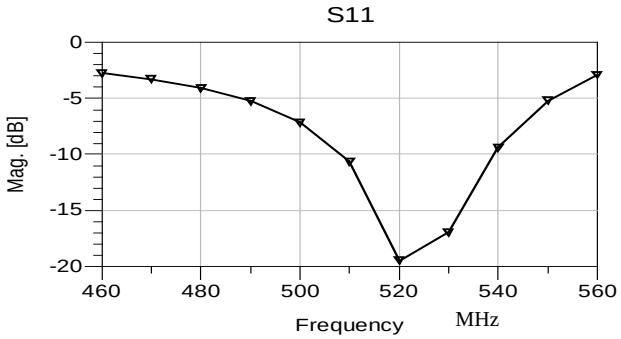

FIGURE 21. FOLDED ANTENNA WITH SRR, COMPUTED S11

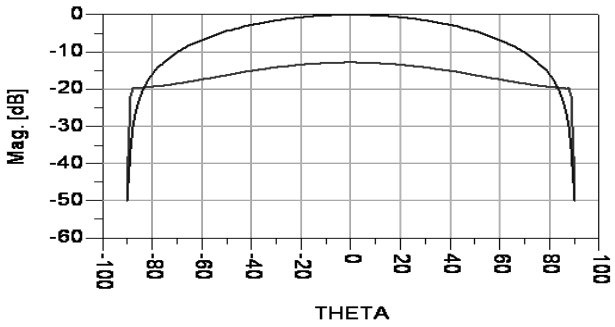

FIGURE 22. RADIATION PATTERN OF THE FOLDED ANTENNA WITH SRR

The computed S11 parameter of the modified antenna with metallic strips is presented in Figure 19. The antenna bandwidth is around 50% for VSWR better than 2.3:1.

The size of the antenna shown in Figure 6 may be reduced by folding the printed dipole as shown in Figureure 20. The dimensions of the folded dual polarized antenna with SRR presented in Figure 20 are 11x11x0.16cm. The antenna bandwidth is 10% for VSWR better than 2:1.

Figure 21 presents the antenna computed S11 parameters.
The computed radiation pattern of the folded antenna with SRR is shown in Figure 22.

Stacked Patch Antenna Loaded With Split Ring Resonators

At first a microstrip stacked patch antenna [3] has been designed. The second step was to design the same antenna with Split Ring Resonators. The antenna consists of two layers. The first layer consists of FR4 1.6mm dielectric substrate with dielectric constant of 4. The second layer consists of RT-DUROID 5880 1.6mm dielectric substrate with dielectric constant of 2.2. The dimensions of the microstrip stacked patch antenna shown in Figure 23 are 33x20x0.32mm. The antenna has been analyzed by using Agilent ADS software. The antenna bandwidth is around 5% for VSWR better than 2.5:1. The antenna beam width is around 72º. The antenna gain is around 7dBi. The computed S11 parameters are presented in Figure 24. Radiation pattern of the microstrip stacked patch is shown in Figure 25. The antenna with Split Ring Resonators is shown in Figure 26. This antenna has the same structure as the antenna shown in Figure 23. The ring width is 0.2mm the spacing between the rings is 0.25mm. Twenty eight SRR are placed on the radiating element. There is a good agreement between measured and computed results. The computed S11 parameters of the antenna with SRR are presented in Figure 26. The antenna bandwidth is around 5% for VSWR better than 2.5:1. The antenna gain is around 10dBi. The antenna computed radiation pattern is shown in Figure 27.

The antenna beam width is around 70º. The gain and directivity of the stacked patch antenna with SRR is higher by 2.5dB than patch the antenna without SRR.

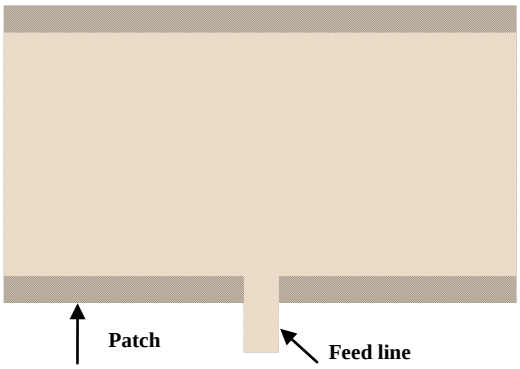

FIGURE 23. A MICROSTRIP STACKED PATCH ANTENNA

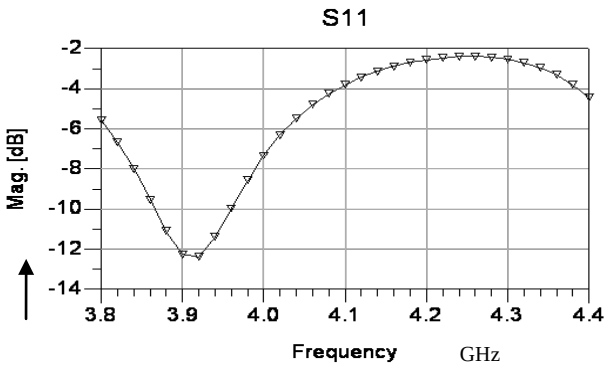

FIGURE 24. COMPUTED S11 OF THE MICROSTRIP STACKED PATCH

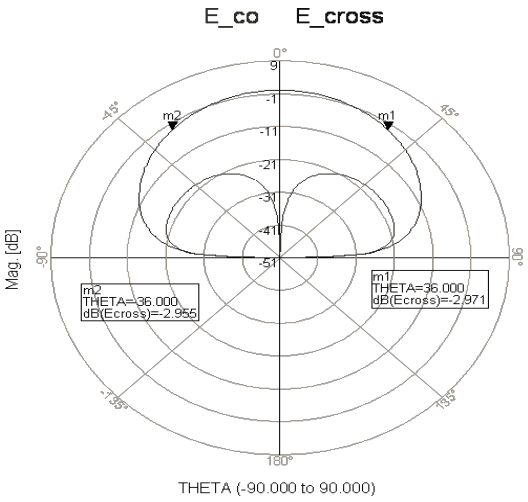

FIGURE 25. RADIATION PATTERN OF THE MICROSTRIP STACKED PATCH

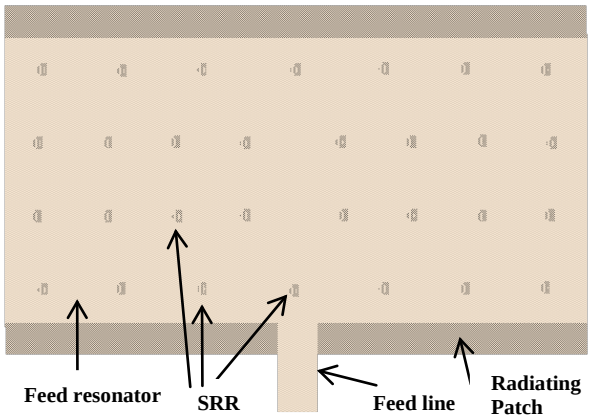

FIGURE 26. PRINTED ANTENNA WITH SPLIT RING RESONATORS

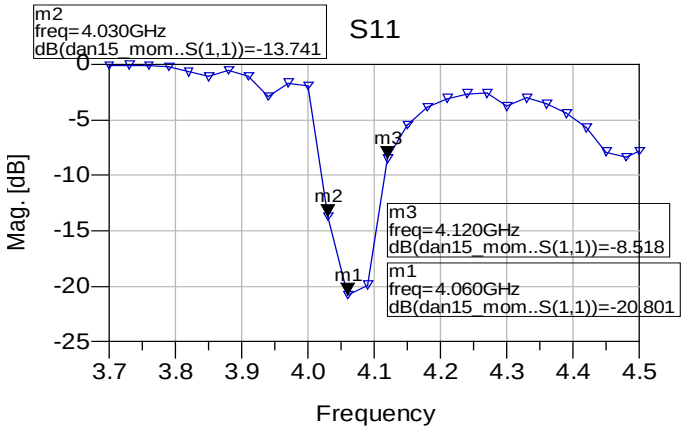

FIGURE 27. ANTENNA WITH SPLIT RING RESONATORS, COMPUTED S11

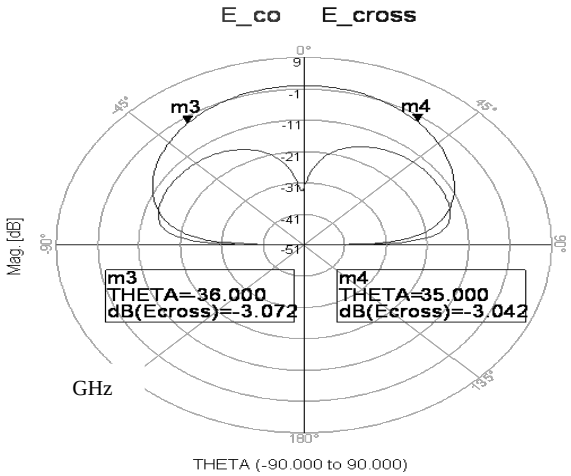

FIGURE 28. RADIATION PATTERN FOR PATCH WITH SRR

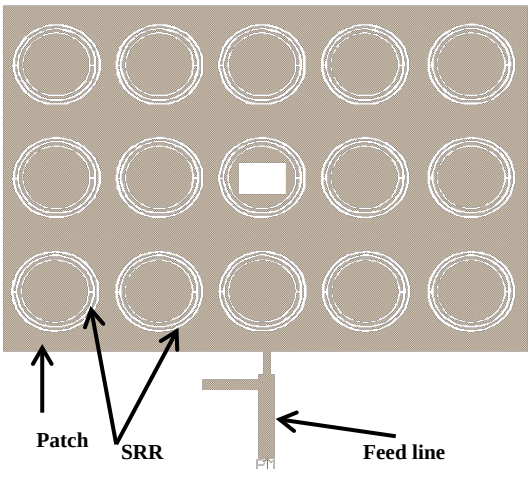

FIGURE 28. PATCH ANTENNA WITH SPLIT RING RESONATORS

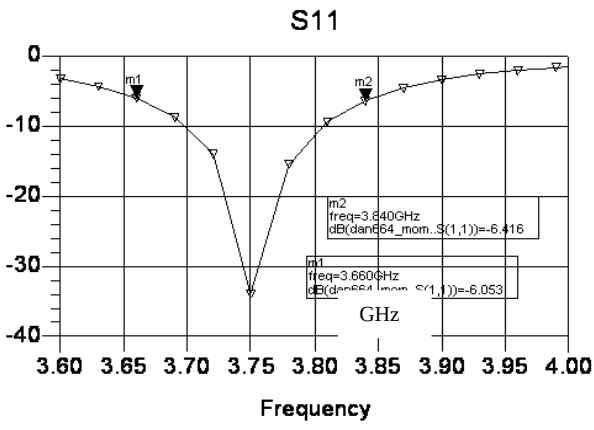

FIGURE 29. PATCH WITH SPLIT RING RESONATORS, COMPUTED S11

Patch Antenna Loaded With Split Ring Resonators

A patch antenna with Split Ring Resonators has been designed. The antenna is printed on RT-DUROID 5880 1.6mm dielectric substrate with dielectric constant of 2.2. The dimensions of the microstrip patch antenna shown in Figure 28 are 36x20x0.32mm. The antenna bandwidth is around 4% for VSWR better than 2:1. The antenna beam width is around 72º. The antenna gain is around 7dBi. The computed S11 parameters are presented in Figure 29.The gain and directivity of the patch antenna with SRR is higher by 2.5dB than patch the antenna without SRR.

TABLE 1 PROPERTIES OF HUMAN BODY TISSUES

Tissue	Property	434 MHz	600 MHz
Skin	σ	0.57	0.6
	ε	41.6	40.43
Stomach	σ	0.67	0.73
	ε	42.9	41.41
Colon, Muscle	σ	0.98	1.06
	ε	63.6	61.9
Lung	σ	0.27	0.27
	ε	38.4	38.4

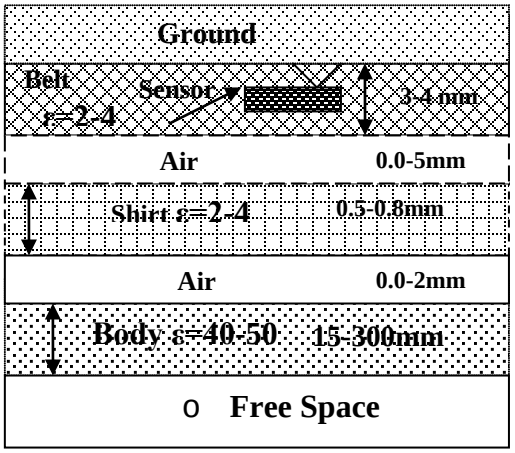

FIGURE 30. ANALYZED STRUCTURE FOR IMPEDANCE COMPUTATIONS

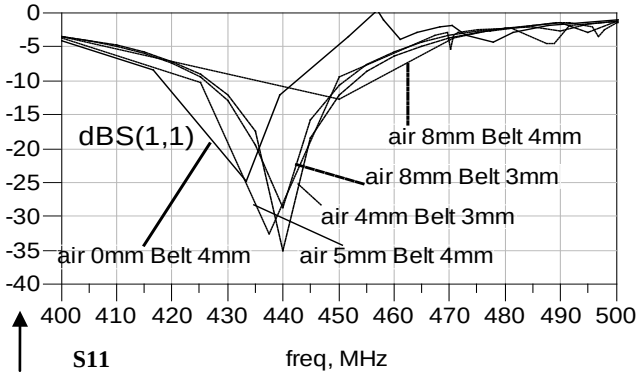

FIGURE 31. S11 RESULTS OF THE ANTENNA WITH DIFFERENT THICKNESSES AND SPACING RELATIVE TO THE HUMAN BODY

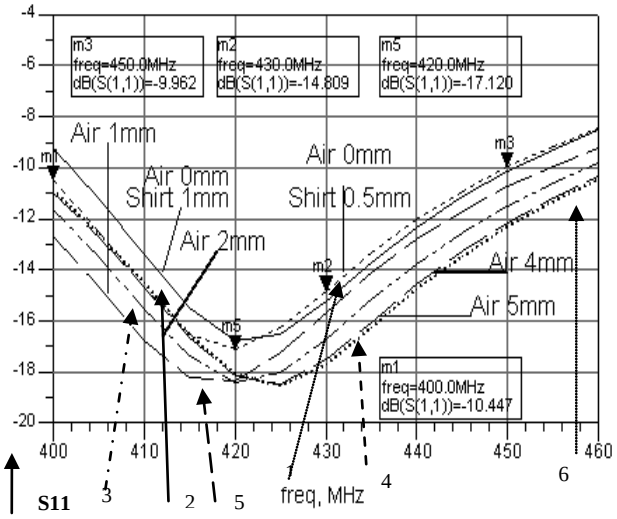

FIGURE 32. FOLDED ANTENNA S11 RESULTS FOR DIFFERENT ANTENNA POSITION RELATIVE TO THE HUMAN BODY

TABLE 2 EXPLANATION OF FIGURE 32

Picture #	Line type	Sensor position
1	Dot ·····	Shirt thickness 0.5mm
2	Line ——	Shirt thickness 1mm
3	Dash dot -·-·-	Air spacing 2mm
4	Dash - - - -	Air spacing 4mm
5	Long dash — —	Air spacing 1mm
6	Big dots •••••	Air spacing 5mm

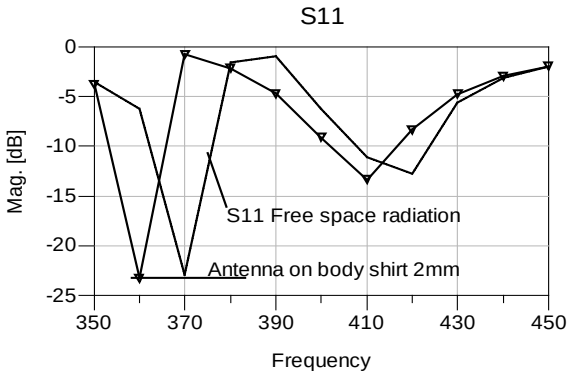

FIGURE 33. S11 OF THE ANTENNA WITH SRR ON THE HUMAN BODY

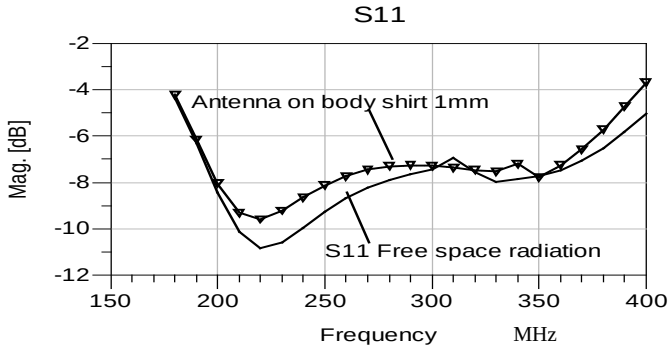

FIGURE 34. ANTENNA WITH SRR S11 RESULTS ON THE HUMAN BODY

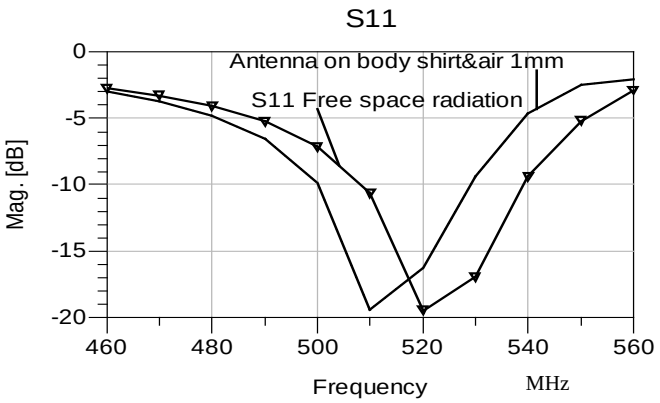

FIGURE 35. FOLDED ANTENNA WITH SRR S11, ON THE HUMAN BODY

Antenna S11 Varitaion as Function of the Distance from Human Body

The Antennas input impedance variation as function of distance from the body had been computed by employing ADS software. The analyzed structure is presented in Figure 30. The patient body thickness was varied from 15mm to 300mm. The location of the antenna on human body may be taken into account by calculating S11for different dielectric constant of the body. The variation of the dielectric constant of the body from 40 to 60 shifts the antenna resonant frequency up to 2%. The antenna was placed inside a belt with thickness between 2 to 4mm with dielectric constant from 2 to 4. The air layer between the belt and the patient shirt may vary from 0mm to 8mm. The shirt thickness was varied from 0.5mm to 1mm. The dielectric constant of the shirt was varied from 2 to 4. Properties of human body tissues are listed in Table 1 see [15]. These properties were employed in the antenna design.

Figure 31 presents S11 results (of the antenna shown in Figure 1). For different belt thickness, shirt thickness and air spacing between the antennas and human body. One may conclude from results shown in Figure 31 that the antenna has V.S.W.R better than 2.5:1 for air spacing up to 8mm between the antennas and the human body. Results shown in Figure 31 indicates that the antenna has V.S.W.R better than 2.0:1 for air spacing up to 5mm between the antennas and patient body. Figure 32 presents S11 results for different position relative to the human body of the folded antenna shown in Figure 4. Explanation of Figure 32 is given in Table II. If the air spacing between the sensors and the human body is increased from 0mm to 5mm the antenna resonant frequency is shifted by 5%. A voltage controlled varactor may be used to control the wearable antenna resonant frequency at different locations on the human body as presented in [25]. Figure 33 presents S11 results of the antenna with SRR shown in Figure 8 on the human body. The antenna resonant frequency is shifted by 3%. Figure 34 presents S11 results of the antenna with SRR, shown in Figure 18, on the human body. The antenna resonant frequency is shifted by 1%. Figure 35 presents S11 results of the folded antenna with SRR shown in Figure 8 on the body. The antenna resonant frequency is shifted by 2%. The radiation pattern of the folded antenna with SRR on human body is presented in Figure 36.

Wearable Antennas

An application of the proposed antenna is shown in Figure 37. Three to four folded dipole or loop antennas may be assembled in a belt and attached to the patient stomach. The cable from each antenna is connected to a recorder. The received signal is routed to a switching matrix. The signal with the highest level is selected during the medical test. The antennas receive a signal that is transmitted from various positions in the human body. Folded antennas may be also attached on the patient back in order to improve the level of the received signal from different locations in the human body. In several applications the distance separating the transmitting and receiving antennas is less than $2D^2/\lambda$. D is the largest dimension of the radiator. In these applications the amplitude of the electromagnetic field close to the antenna may be quite powerful, but because of rapid fall-off with distance, the antenna do not radiate energy to infinite distances, but instead the radiated power remain trapped in the region near to the antenna. Thus, the near-fields only transfer energy to close distances from the receivers. Change in current flow through one wire induces a voltage across the ends of the other wire through electromagnetic induction. The amount of inductive coupling between two conductors is measured by their mutual inductance. In these applications we have to refer to

the near field and not to the far field radiation. The antennas radiation characteristics on human body have been measured by using a phantom. The phantom electrical characteristics represent the human body characteristics.

The phantom has a cylindrical shape with a 40cm diameter and a length of 1.5m. The phantom contains a mix of 55% water 44% sugar and 1% salt. The antenna under test was placed on the phantom during the measurements of the antennas radiation characteristics. In Figure 38 to 39 several photos of printed antennas for medical applications at 434MHz are shown. The dimensions of the folded dipole antenna are 7x6x0.16cm. The dimensions of the compact folded dipole presented in Figure 37 are 5x5x0.5cm.

Small Metamaterial Antennas Analysis

By employing the analysis of small antennas given by James S. Mclean we can calculate the bandwidth of small antennas loaded with SRR. A small antenna is defined as an antenna who's maximum dimension is less than $\frac{\lambda}{2\pi}$ or $\frac{\lambda}{2\pi}a < 1$.

The free space wavelength is λ . The radius of sphere enclosing the maximum dimension of the antenna is a. For an electrically small antenna, contained within a given volume, the antenna has a minimum value of Q [27]. This places a limit on the attainable impedance bandwidth of an Electrically Small Antenna, ESA. The minimum Q for an electrically small linear antenna in free space is expressed as (1): $Q = \frac{1}{k^3a^3} + \frac{1}{\mathrm{ka}}$ (1). The gain of a small antenna is bounded and is given as (2):

$$G = k^2a^2 + 2\mathrm{ka} \tag{2}$$

Equation (2) may be solved as a quadratic equation where $\boldsymbol{a}$ represents an unknown for a given gain G.

$$0 = k^2a^2 + 2\mathrm{ka} - \mathrm{G} \tag{3}$$

The solution of (3) is given by (4):

$$a = \frac{-1 + \sqrt{1+G}}{2\pi}\lambda \tag{4}$$

For an efficient small meta-material antenna the effective antenna area is greater than the antenna physical area and may be written as in (5), a_M .

$$a_M = \frac{-1 + \sqrt{1+G_M}}{2\pi}\lambda \tag{5}$$

The gain of the efficient small antenna may be written as $G_{M=}G\alpha_M > G$. Q_{LM} for a small efficient antenna may be expressed as given in (6).

$$Q_{LM} = \frac{1}{k^3\mathrm{a}_M^3} + \frac{1}{\mathrm{ka}_M} \tag{6}$$

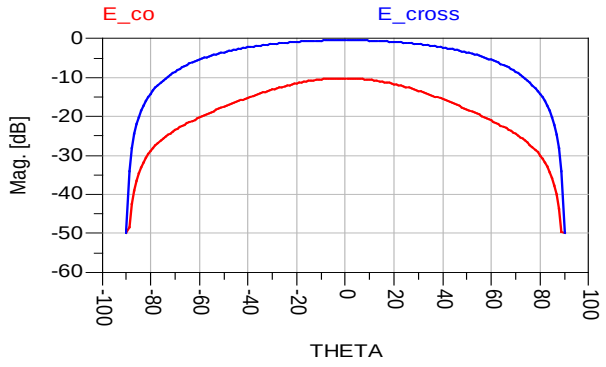

FIGURE 36. RADIATION PATTERN OF THE FOLDED ANTENNA WITH SRR ON HUMAN BODY

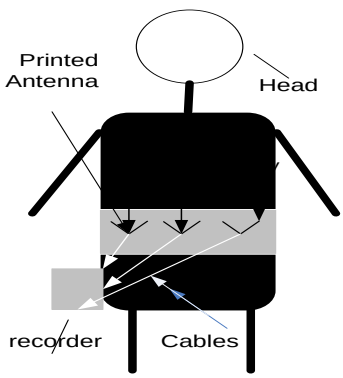

FIGURE 37. MEDICAL SYSTEM WITH PRINTED WEARABLE ANTENNA

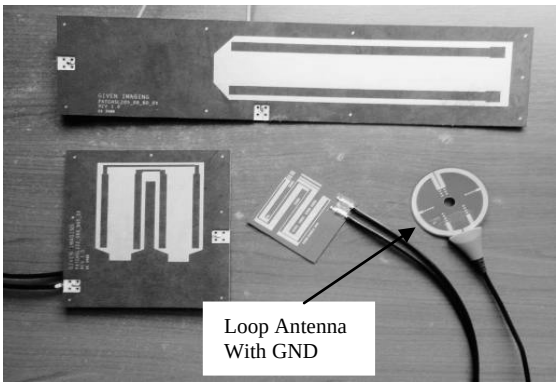

FIGURE 38. MICROSTRIP ANTENNAS FOR MEDICAL APPLICATIONS

FIGURE 39. METAMATERIAL ANTENNAS FOR MEDICAL APPLICATIONS

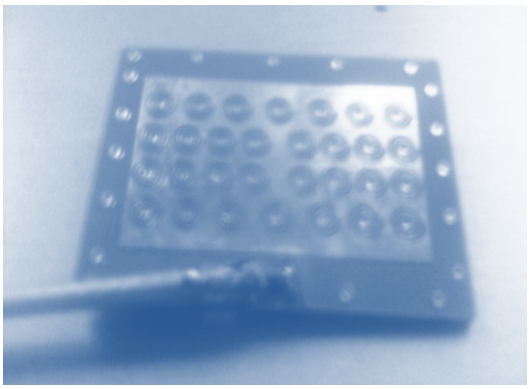

FIGURE 40. METAMATERIAL PATCH ANTENNA

TABLE 2 COMPUTED BANDWIDTH OF SMALL ANTENNAS

Frequency (MHz)	K(rad/m)	a (cm)	ka	G (dB)	QL	BW%
400	8.37	10	0.84	3.75	2. 90	24.37
450	9.42	8	0.75	3.2	3.66	19.31

TABLE 3 COMPUTED BANDWIDTH OF SMALL ANTENNAS WITH SRR

Freq. (MHz)	ka(rad/m)	a_M(cm)	ka_M	G (dB)	Q_{LM}	BW%
400	8.37	12.40	1.04	5	1.85	38.21
300	6.28	16.55	1.04	5	1.85	38.21

For a given VSWR S the antenna bandwidth BW may be written as (7):

$$BW = \frac{S-1}{Q_{LM}\sqrt{S}} \tag{7}$$

Q_{LM} can be expressed as (8):

$$Q_{LM} = \frac{S-1}{BW\sqrt{S}} \tag{8}$$

Computed values of small antennas are given in Table 2. Computed values of antennas with SRR are given in Table 3. Table 3 indicates that the bandwidth of small antennas with SRR may be wider than the bandwidth of small antennas without SRR.

Conclusions

Meta material technology is used to develop small antennas with high efficiency. A new class of printed meta-materials antennas with high efficiency is presented in this paper. The bandwidth of the antenna with SRR and metallic strips is around 50% for VSWR better than 2.3:1. Optimization of the number of the coupling stubs and the distance between the coupling stubs may be used to tune the antenna resonant frequency and number of resonant frequencies. The gain and directivity of the patch antenna with SRR is higher by 2.5dB than the patch antenna without SRR. The resonant frequency of the antenna with SRR on human body is shifted by 3%.

REFERENCES

[1] J.R. James, P.S Hall and C. Wood, "Microstrip Antenna Theory and Design",1981.

[2] Sabban and K.C. Gupta, "Characterization of Radiation Loss from Microstrip Discontinuities Using a Multiport Network Modeling Approach", I.E.E.E Trans. on M.T.T, Vol. 39,No. 4,April 1991, pp. 705-712.

[3] Sabban," A New Wideband Stacked Microstrip Antenna", I.E.E.E Antenna and Propagation Symp., Houston, Texas, U.S.A, June 1983.

[4] Sabban, "Microstrip Antenna Arrays", Microstrip Antennas, Nasimuddin Nasimuddin (Ed.), ISBN: 978-953-307-247-0, InTech, http://www.intechopen.com/articles/show/title/microstrip-antenna-arrays , pp. 361-384, 2011.

[5] Sabban, 'New Wideband printed Antennas for Medical Applications" I.E.E.E Journal, Trans. on Antennas and Propagation, Vol. 61, No. 1, pp. 84-91, January 2013.

[6] J. B. Pendry, A. J. Holden, W. J. Stewart, and I. Youngs "Extremely low frequency plasmons in metallic mesostructures." Phys. Rev. Lett., vol. 76, pp. 4773–4776, 1996

[7] J. B. Pendry, A. J. Holden, D. J. Robbins, and W. J. Stewart "Magnetism from conductors and enhanced nonlinear phenomena." IEEE Trans. Microwave Theory Tech., vol. 47, pp. 2075–2084, 1999.

[8] R. Marque´s, F. Mesa, J. Martel, and F. Medina "Comparative analysis of edge and broadside coupled split ring resonators for metamaterial Design Theory and Experiment." IEEE Trans. Antennas Propag., Vol. 51, pp. 2572–2581, 2003.

[9] R. Marque´s, J. D. Baena, J. Martel, F. Medina, F. Falcone, M. Sorolla, and F. Martin "Novel small resonant electromagnetic particles for metamaterial and filter design." Proc. ICEAA'03, pp. 439–442, Torino, Italy, 2003.

[10] R. Marque´s, J. Martel, F. Mesa, and F. Medina "Left-handed-media simulation and transmission of EM waves in subwavelength split-ring-Resonator-loaded metallic waveguides." Phys. Rev. Lett., vol. 89, paper 183901, 2002

[11] J. D. Baena, R. Marque´s, J. Martel, and F. Medina "Experimental results on metamaterial simulation using SRR-loaded waveguides." Proc. IEEE-AP/S Int. Symp. on Antennas and Propagation, pp. 106–109, 2003

[12] R. Marque´s, J. Martel, F. Mesa, and F. Medina "A new 2-D isotropic left- handed metamaterial design: theory and experiment." Microwave Opt. Tech. Lett. vol. 35, pp. 405–408, 2002

[13] R. A. Shelby, D. R. Smith, S. C. Nemat-Nasser, and S. Schultz "Microwave transmission through a two-dimensional, isotropic, left-handed Metamaterial." Appl. Phys. Lett., vol. 78, pp. 489–491, 2001

[14] Jiang Zhu and G. V. Eleftheriades, "A Compact Transmission-Line Metamaterial antenna with Extended Bandwidth", IEEE Antennas and Wireless Propagation Letters Vol. 8, 2009.

[15] Lawrence C. Chirwa*, Paul A. Hammond, Scott Roy, and David R. S. Cumming, "Electromagnetic Radiation from Ingested Sources in the Human Intestine between 150 MHz and 1.2 GHz", IEEE Transaction on Biomedical eng., VOL. 50, NO. 4, April 2003, pp 484-492.

[16] D.Werber, A. Schwentner, E. M. Biebl, "Investigation of RF transmission properties of human tissues", Adv. Radio Sci., 4, 357–360, 2006.

[17] Gupta, B., Sankaralingam S., Dhar, S.,"Development of wearable and implantable antennas in the last decade", Microwave Symposium (MMS), 2010 Mediterranean 2010 , Page(s): 251 – 267.

[18] Thalmann T., Popovic Z., Notaros B.M, Mosig, J.R.," Investigation and design of a multi-band wearable antenna", 3rd European Conference on Antennas and Propagation, EuCAP 2009. Pp. 462 – 465.

[19] Salonen, P., Rahmat-Samii, Y., Kivikoski, M.," Wearable antennas in the vicinity of human body", IEEE Antennas and Propagation Society International Symposium, 2004. Vol.1 pp. 467 – 470.

[20] Kellomaki T., Heikkinen J., Kivikoski, M., " Wearable antennas for FM reception", First European Conference on Antennas and Propagation, EuCAP 2006 , pp. 1-6.

[21] A. Sabban, "Wideband printed antennas for medical applications" APMC 2009 Conference, Singapore, Dec. 2009.

[22] A. Alomainy, A. Sani et all "Transient Characteristics of Wearable Antennas and Radio Propagation Channels for Ultrawideband B ody-centric Wireless Communication", I.E.E.E Trans. on Antennas and Propagation, Vol. 57, No. 4, April 2009, pp. 875-884.

[23] M. Klemm and G. Troester, "Textile UWB antenna for Wireless Body Area Networks", ", I.E.E.E Trans. on Antennas and Propagation, Vol. 54, No. 11, Nov. 2006, pp. 3192-3197.

[24] P. M. Izdebski, H. Rajagoplan and Y. Rahmat-Sami, " Conformal Ingestible Capsule Antenna: A Novel Chandelier Meandered Design",", I.E.E.E Trans. on Antennas and Propagation, Vol. 57, No. 4, April 2009, pp. 900-909.

[25] A. Sabban, "Wideband Tunable Printed Antennas for Medical Applications", I.E.E.E Antenna and Propagation Symp., Chicago IL. , U.S.A, July 2012.

[26] A. Sabban, "Wearable Antennas for Medical Applications" In IEEE BodyNet 2013, Boston U.S.A, 2013, pp. 1-7.

[27] James S. Mclean, "A Rexamination of the fundamental Limits of the Radiation Q of the Electrically Small Antennas", I.E.E.E, Trans. on Antennas and Propagation, Vol. 44, No. 5, pp. 672-675, January 1996.

A. Sabban (M'87-SM'94) received the B.Sc degree and M.Sc degree Magna Cum Laude in electrical engineering from Tel Aviv University, Israel in 1976 and 1986 respectively. He received the Ph.D. degree inngineering electrical e from Colorado University at Boulder, USA, in 1991. Dr. A. Sabban reasearch interests are microwave and antenna engineering.

In 1976 he joined the armament development authority RAFAEL in Israel. In RAFAEL he worked as a senior researcher, group leader and project leader in the electromagnetic department till 2007. In 2007 he retired from RAFAEL. From 2008 to 2010 he worked as an RF Specialist and project leader in Hitech companies. From 2010 to date he is a senior lecturer and researcher in Ort Braude College in Israel in the electrical engineering department. He published over 60 research papers and hold a patent in the antenna area.